Numerical simulation of blood pulsatile flow in stenotic coronary arteries: The effect of turbulence modeling and non-Newtonian assumptions

Violeta Carvalho
Department of Production and Systems
University of Minho
Guimarães, Portugal
violetacarvalho_97@hotmail.com

Nelson Rodrigues
ALGORITMI Research Centre
University of Minho
Guimarães, Portugal
nelson.rodrigues@dps.uminho.pt

Rui A. Lima
MEtRICs Research Centre
University of Minho
Guimarães, Portugal
rl@dem.uminho.pt

Senhorinha Teixeira
ALGORITMI Research Centre
University of Minho
Guimarães, Portugal
st@dps.uminho.pt

***Abstract*— Atherosclerosis is a common cardiovascular disease characterized by the accumulation of plaques on the artery walls, resulting in the lumen stenosis. Over the past few decades, this pathological condition has been deeply studied and computational fluid dynamics has played an important role in investigating the blood flow behavior. Commonly, the blood flow is assumed to be laminar and a Newtonian fluid. However, under a stenotic condition, the blood behaves as a non-Newtonian fluid and the pulsatile blood flow through coronary arteries could result in a transition from laminar to turbulent flow condition. The aim of the present study is to analyze and compare numerically by means of CFD the blood flow behavior, applying the k-ω SST model and a laminar assumption. The effects of Newtonian and non-Newtonian (Carreau) models were also studied.**

According to the results, the turbulent model is shown to give a better overall representation of pulsatile flow in stenotic arteries. In addition, the effect of non-Newtonian modeling was found to be more significant in wall shear stress measurements than in velocity profiles.

Keywords—hemodynamics, CFD, atherosclerosis, turbulence, non-Newtonian, coronary arteries

I. INTRODUCTION

Cardiovascular diseases (CVDs) are the leading cause of death globally, being expected to cause over 22 million deaths per year in 2030. The main underlying pathological process of CVDs is atherosclerosis, an inflammatory disorder of the arterial wall, which narrows its lumen [1]. During early stages, there are no significant changes in the flow dynamics, nevertheless, as time progresses, these plaques play a critical role in altering the flow characteristics and transition to turbulence can occur, even at much lower Reynolds number [2], [3]. To understand the flow field changes, several hemodynamic studies have been conducted. This can be achieved under *in vivo* conditions using different measurement techniques. However, it is difficult to measure with sufficient accuracy some hemodynamic parameters, e.g wall shear stress (WSS). For this reason, computational fluid dynamics (CFD) has been used as an effective alternative to investigate in detail several blood flow phenomena in blood vessels and an important component in the study of CVDs, allowing the calculation of various hemodynamic parameters with high precision [2], [4].

One of the earliest detailed studies of the flow in stenosis was conducted by Young [5] considering the flow in a mildly constricted tube based on a simplified model. Over the years, research into hemodynamics has grown exponentially and researchers have taking different assumptions, because of the blood flow complexity. Some authors assumed the blood flow in coronary arteries to be laminar [6]–[11] and behave as Newtonian fluid [9], [12]–[14], and others studied turbulence transition [2], [3], [15]–[17] and non-Newtonian effects [2], [7], [18]. In fact, in large vessels, blood can be considered as a homogeneous fluid with constant viscosity. However, in the presence of stenosis, it is observed that the viscosity decreases with increasing velocity and reduction of vessel diameter. Therefore, the non-Newtonian behavior should be considered [10]. Another important factor to the local hemodynamics is the shape of the stenosis. Some researchers apply idealized stenosis shapes [14], [18], [19], while others make use of artery stenotic models based on medical images [6], [20], [21]. For instance, Gaudio et al [10] compared Newtonian and non-Newtonian (Carreau-Yasuda model) blood behaviors in patient-specific stenotic coronary arteries at different degrees of stenosis. For that, the researchers investigated numerically the blood velocity and the distribution of the shear stress indices at different times of the cardiac cycle. Their results showed that the velocity for the Carreau-Yasuda model is slightly lower when compared to the Newtonian model, however, the non-Newtonian effects are most important in shear stress indices distributions. Kamangar and his team [21] investigated the effect of stenosis in left coronary arteries on the hemodynamics in suspected diseased patients, using non-Newtonian (Carreau model) and laminar assumptions. They observed a considerable pressure drop and an increase in the velocity and wall shear stress at the stenosis throat. In the post stenotic section, they observed the prevalence of a recirculation zone which can result in the growth or formation of a new stenosis.

To understand the turbulence transition effect on hemodynamic parameters, Mahalingam et al. [2] applied the SST k-ω model during pulsatile flow through coronary arteries for different degrees of stenosis. They demonstrated that the transition to turbulence starts occurring above 50% stenosis and becomes fully turbulent above and beyond 70% of stenosis.

According to the literature, the best suited turbulent model to simulate the blood flow in pulsatile conditions is

2020 24th International Conference on Circuits, Systems, Communications and Computers (CSCC) | 978-1-7281-6503-5/20/$31.00 ©2020 IEEE | DOI: 10.1109/CSCC49995.2020.00027

978-1-7281-6503-5/20/$31.00 ©2020 IEEE
DOI 10.1109/CSCC49995.2020.00027

the transitional k-ω model, also referred as SST k-ω. This has been investigated and validated by several authors [3], [16], [17], [22] using as reference the experimental study of Ahmed and Giddens [23]. However, the comparison between laminar and turbulent modeling has not been greatly investigated and the selection of the proper models to simulate the blood flow is vital to ensure the accuracy and reliability of numerical results. This is of great importance, since the objective of hemodynamic numerical studies is to simulate as best as possible the phenomena that occur *in vivo*.

In this regard, in the current study an analysis of the turbulence modeling effects on blood flow is performed, comparing the SST k-ω model to a laminar flow in an idealized coronary artery with 70% of stenosis. Additionally, the effect of shear-thinning blood behavior was also studied, by using the Carreau model.

II. Methodology

A. Geometry of the stenotic coronary artery model

To study the blood flow, it is necessary to obtain the three-dimensional geometry of the lumen of the coronary artery. This step was performed in the Design Modeler tool in ANSYS® workbench. The selected diameter was based on real data obtained in the literature [24], and according to some authors [2], [25], [26], the length of the stenosis is defined as twice the normal diameter. In addition, the entrance length was chosen so that the velocity profiles could be fully established proximal to the stenosis. The axisymmetric stenosis model developed, and its geometric parameters are represented in Fig. 1.

B. Mesh generation and blood flow assumptions

The numerical meshing and simulations were performed in the computational fluid dynamics (CFD) package ANSYS Fluent (version R2). In Ansys Meshing, a hexahedral mesh was created with a bias factor to ensure the accuracy of computational calculations near the wall, and a more refined mesh in the stenotic section (Fig. 1). To assure a mesh independent solution, grid tests were made by refining the mesh and rerunning the simulations until no significant differences were observed. The results were mesh-independent after using a grid of 510,720 elements.

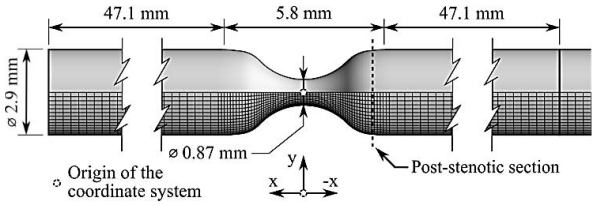

Fig. 1. Geometry and dimensions of the 70% stenotic model with the generated mesh represented at the half bottom of the figure.

Blood flow is modeled using the Navier-Stokes and the continuity equations as follows in Equation 1 and 2,

$$\nabla \cdot \vec{u} = 0 \tag{1}$$

$$\rho\left(\frac{\partial \vec{u}}{\partial t} + \vec{u} \cdot \nabla\right) = -\nabla p + \mu \nabla^2 \vec{u} \tag{2}$$

where $\vec{u}$ is the velocity vector, p is the static pressure, ρ is the fluid density, and μ the dynamic viscosity . These were solved by the semi-implicit method for pressure linked equations (SIMPLE) scheme.

To ensure that this analysis reflects the realistic simulation of *in vivo* conditions, a physiological inlet velocity profile adopted by Doutel et al. [6] was applied. The mean inlet velocity (V_m) of the cardiac cycle is defined as shown in Equation 3, where $\overline{V_m}$ is the average velocity along the cycle, w is the angular frequency of the cardiac cycle, and a_i and b_i are parameters of the fitting model and they were obtained from [6].

$$V_m(t) = \frac{\overline{V_m}}{a_0}\left\{a_0 + \sum_{i=1}^{5}[a_i cos(iwt) + b_i sin(iwt)]\right\} \tag{3}$$

Equation 3 was written in C-language using the interface of User Defined Function (UDF) of Fluent and linked with the solver. For each transient simulation, four consecutive cardiac cycles were run and the results from the last cycle were analyzed.

When the blood is modeled as a Newtonian fluid, appropriate rheological parameters were applied with a density of 1072.033 $kg \cdot m^{-3}$ and a viscosity of 0.00315 $Pa \cdot s$, which are similar to those used in previous studies [6], [11], [27]. For the pulsatile non-Newtonian blood flow simulations, the selected viscosity model was the Carreau, since it is commonly used by several authors [6], [7], [28] to simulate the shear-thinning blood behavior and it is considered the most suitable to perform these simulations. In the Carreau model, the viscosity (μ) is given by Equation 4,

$$\mu = \mu_\infty + (\mu_0 - \mu_\infty)[1 + \lambda\dot{\gamma}^2]^{\frac{n-1}{2}} \tag{4}$$

where, according to the previously cited authors, $\mu_\infty = 0.00345\ Pa \cdot s$ is the infinite shear viscosity, $\mu_0 = 0.0560\ Pa \cdot s$ is the blood viscosity at zero shear rate, $\dot{\gamma}$ is the instantaneous shear rate, $\lambda = 3.313\ s$ is the time constant and $n = 0.3568$ is the power-law index.

In addition, the artery walls were considered as rigid with a no-slip condition. For incompressible fluids, spatial WSS, τ_w, is calculated by Equation 5, being $\dot{\gamma}$, the deformation rate.

$$\tau_w = \mu\frac{\partial u}{\partial y} = \mu\dot{\gamma} \tag{5}$$

C. Turbulence modeling: Transitional k-ω model

Turbulent models include variations to the governing equations to capture the turbulent fluctuations in the flow field, and these are calculated through Equation 6 and 7.

$$\frac{\partial(\rho\bar{u}_i)}{\partial x_i} = 0 \tag{6}$$

$$\frac{\partial \rho\bar{u}_i}{\partial t} + \frac{\partial}{\partial x_j}\left(\rho\bar{u}_i\bar{u}_j + \rho\overline{u'_i u'_j}\right) = -\frac{\partial \bar{p}}{\partial x_i} + \frac{\partial \overline{\bar{\tau}_{ij}}}{\partial x_j} \tag{7}$$

The transitional k-ω model is similar to the standard model, but with some modifications. The SST k-ω model has two other transport equations, one for the intermittency and one for the transition onset criteria. This is of interest in this study since the flow is not fully turbulent in the entire domain or throughout the entire cardiac cycle [3], [17]. Moreover, this model is used to effectively combine the robust and accurate formulation of the k-ω model in the near-wall regions with the freestream independence of the k-ε model far from the wall [3], [29], [30]. The transport equations for the turbulent kinetic energy, k, and the specific dissipation rate, ω are modeled as follows in Equations 8 and 9.

G_k represents the generation of turbulence kinetic energy due to mean velocity gradients, G_ω represents the generation of ω. r_ω and r_k represent the effective diffusivity of k and ω, respectively. Y_k and Y_ω represent the dissipation of k and ω due to turbulence. D_ω represents the cross-diffusion term. S_k and S_ω are user-defined source terms.

III. Results and Discussion

A. Turbulent models and laminar comparison

To assess the flow behavior through the simulated stenotic artery, a velocity profile of the fluid flow was plotted along the geometry center. The plotted data starts near the stenosis center, where X = 0 and follows the blood flow direction until X = -50 mm. Fig.2 I) and II) represent the velocity flow in the diastolic and systolic peak, respectively, assuming the blood as a Newtonian fluid. For both phases, the effect of the laminar and turbulent behavior according to the SST k-ω model was studied.

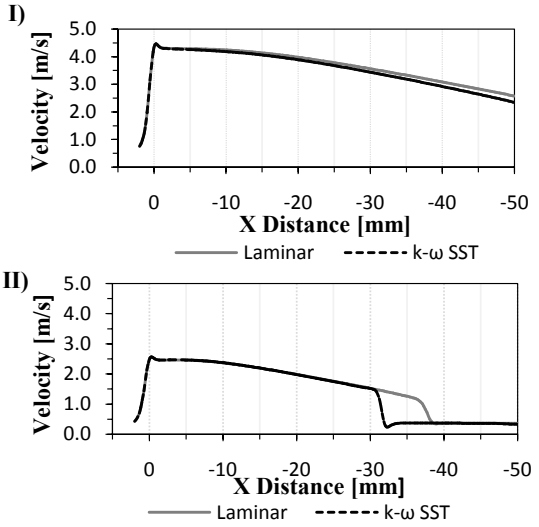

Fig. 2. Simulated centerline velocity at the time of the: I) diastolic peak; II) systolic peak of the input velocity profile.

Through observation of Fig. 2, it is possible to observe that the velocity waveform and the predicted values near and at the stenosis throat (X = 0) by both models in the different phases of the cardiac cycle are in excellent agreement. However, after the contraction, the differences are more notable. In the diastolic peak (Fig.2 I), the SST k-ω and laminar model show a similar behavior along the geometry, with a gradual reduction in velocity after stenosis. These results are in good agreement with a study conducted by Straatman et al. [17], who also compared the SST k-ω model with experimental data obtained by Ahmed and Giddens [23]. Looking at Fig.2 II, it can be also observed an identical behavior for both models, however, the transitional k-ω model presents an earlier drop in velocity, that marks the end of the recirculation zone. The laminar model predicts a slightly higher recirculation length. In Straatman work [17], it was also showed that the transitional k-ω model over-predict a bit the length of the recirculation when compared to the experimental data. Taking this assumption, it can be concluded that the laminar model over-predicts considerably more the recirculation length, and, therefore is not the most adequate.

$$\frac{\partial}{\partial t}(\rho k) + \frac{\partial}{\partial x_i}(\rho k u_i) = \frac{\partial}{\partial x_j}\left(\mathrm{r}_k \frac{\partial_k}{\partial x_j}\right) + G_k - Y_k + S_k \quad (8)$$

$$\frac{\partial}{\partial t}(\rho \omega) + \frac{\partial}{\partial x_i}(\rho \omega u_i) = \frac{\partial}{\partial x_j}\left(\mathrm{r}_\omega \frac{\partial_\omega}{\partial x_j}\right) + G_\omega - Y_\omega + D_\omega + S_\omega \quad (9)$$

Despite the few differences between the two models, it was showed that the model selection influences the results and the most adequate model seems to be the transitional k-ω. For this reason, the remaining simulations were performed with that model.

B. Newtonian and Non-Newtonian behavior

To compare the non-Newtonian effects in flow behavior, the velocity profiles in the stenotic and post stenotic section (X = -2.5 mm), only at the diastolic peak were evaluated. As it can be observed in Fig. 3 a) and b), the two models

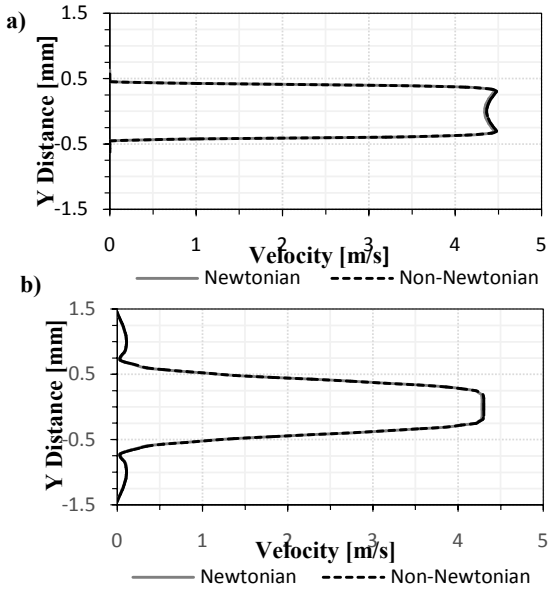

present the same behavior and there is only a small variation in the maximum velocity. It can be seen a lower maximum value in the curve of the Newtonian model compared to the Carreau model.

Fig. 3. Comparison between the velocity profiles at: a) stenotic section; b) the post-stenotic section.

In addition, to evaluate if the differences are significative a statistical analysis was performed by applying a t-test for a significance level, α, of 0.1. The P values obtained were approximately 0.99 for both cases, Fig. 3 a) and b). This shows that there are not significant differences between the two models.

Fig. 4 shows the wall shear stress (WSS) along the coronary artery, in particular in the region of the stenosis at the diastolic peak.

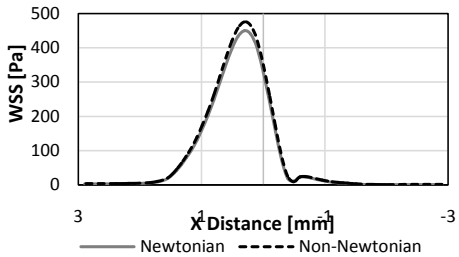

Fig. 4. Comparison between the WSS using the Newtonian and Carreau model.

The maximum value of WSS is located in the maximum narrowing area and the differences between the two models are more perceptible than in velocity. Comparing the Newtonian model to the Carreau model, the first one predicts a lower value of WSS, visible in the peak where there is the presence of the stenosis. These results are in agreement with a previous study conducted by Gaudio et al. [10].

Similarly to the previous results, the t-test was applied in the same conditions, and a P value of 0.82 was obtained. As before, according to the t-test, the differences are not considered significant. However, there is a reasonable difference between the two P values observed, which proves the bigger impact of non-Newtonian assumptions on shear stress measurements.

IV. CONCLUSIONS

The present study provides new insights on the use of the transitional variant of the k-ω model for predicting pulsatile flow through stenotic coronary arteries, instead of the laminar model, which is used commonly by several researchers. Note that, the differences between the two models are verified only in the post stenotic area, where recirculation occurs. The authors also concluded that the non-Newtonian effects are more significant in the wall shear stress measurements, and the Newtonian model predicts lower values. The same tendency was observed in the velocity profiles, however, it is almost imperceptible.

Despite the results agreed with previous studies, further investigations are necessary, because of the complexity of physiological flows.

ACKNOWLEDGMENTS

This work has been supported by FCT – Fundação para a Ciência e Tecnologia within the R&D Units Project Scope: UIDB/00319/2020, UIDP/04077/2020, and NORTE-01-0145-FEDER-030171, funded by COMPETE2020, NORTE 2020, PORTUGAL 2020 and FEDER.

REFERENCES

[1] A. Haverich and E. C. Boyle, *Atherosclerosis Pathogenesis and Microvascular Dysfunction*, First. Springer, 2019.

[2] A. Mahalingam *et al.*, "Numerical analysis of the effect of turbulence transition on the hemodynamic parameters in human coronary arteries," *Cardiovasc. Diagnosis Ther.*, vol. 6, no. 3, pp. 208–220, 2016.

[3] C. Moreno and K. Bhaganagar, "Modeling of stenotic coronary artery and implications of plaque morphology on blood flow," *Model. Simul. Eng.*, vol. 2013, p. 14, 2013.

[4] S. C. P. Cheung *et al.*, "Experimental and numerical study on the hemodynamics of stenosed carotid bifurcation," *Australas. Phys. Eng. Sci. Med.*, vol. 33, no. 4, pp. 319–328, 2010.

[5] D. F. Young, "Effect of a time-dependent stenosis on flow through a tube," *J. Manuf. Sci. Eng. Trans. ASME*, vol. 90, no. 2, pp. 248–254, 1968.

[6] E. Doutel, N. Viriato, J. Carneiro, J. B. L. M. Campos, and J. M. Miranda, "Geometrical effects in the hemodynamics of stenotic and non-stenotic left coronary arteries—numerical and in vitro approaches," *Int. j. numer. method. biomed. eng.*, vol. 35, no. 1, pp. 1–18, 2019.

[7] B. Liu, J. Zheng, R. Bach, and D. Tang, "Influence of model boundary conditions on blood flow patterns in a patient specific stenotic right coronary artery," *Biomed. Eng. Online*, vol. 14, no. Suppl 1, p. S6, 2015.

[8] T. Chaichana, Z. Sun, and J. Jewkes, "Hemodynamic impacts of various types of stenosis inthe left coronary artery bifurcation: A patient-specific analysis," *Phys. Medica*, vol. 29, no. 5, pp. 447–452, 2013.

[9] P. K. Siogkas *et al.*, "Patient-specific simulation of coronary artery pressure measurements: An in vivo three-dimensional validation study in humans," *Biomed Res. Int.*, vol. 2015, p. 628416, 2014.

[10] L. T. Gaudio, M. V. Caruso, S. De Rosa, C. Indolfi, and G. Fragomeni, "Different Blood Flow Models in Coronary Artery Diseases: Effects on hemodynamic parameters," *Proc. Annu. Int. Conf. IEEE Eng. Med. Biol. Soc. EMBS*, vol. 2018-July, pp. 3185–3188, 2018.

[11] V. Carvalho, N. Rodrigues, R. Ribeiro, P. F. Costa, R. A. Lima, and S. F. C. F. Teixeira, "3D Printed Biomodels for Flow Visualization in Stenotic Vessels : An Experimental and Numerical Study," *Micromachines*, vol. 11, no. 6, p. 549, 2020.

[12] M. Biglarian *et al.*, "Computational investigation of stenosis in curvature of coronary artery within both dynamic and static models," *Comput. Methods Programs Biomed.*, vol. 185, p. 105170, 2019.

[13] J. Wu, G. Liu, W. Huang, D. N. Ghista, and K. K. L. Wong, "Transient blood flow in elastic coronary arteries with varying degrees of stenosis and dilatations: CFD modelling and parametric study," *Comput. Methods Biomech. Biomed. Engin.*, vol. 18, no. 16, pp. 1835–1845, 2015.

[14] E. Doutel, J. Carneiro, J. B. L. M. Campos, and J. M. Miranda, "Artificial stenoses for computational hemodynamics," *Appl. Math. Model.*, vol. 59, pp. 427–440, 2018.

[15] S. H. Frankel and S. Varghese, "Numerical Modeling of Pulsatile Turbulent Flow in Stenotic," *J. Biomech. Eng.*, vol. 125, no. 4, pp. 445–460, 2003.

[16] J. Banks, "Turbulence Modeling in Three-Dimensional Stenosed Arterial Bifurcations," *J. Biomech. Eng.*, vol. 129, no. 1, pp. 40–50, 2007.

[17] A. G. Straatman and J. Ryval, "Two-equation Turbulence Modeling of Pulsatile Flow in a," *J. Biomech. Eng.*, vol. 126, no. October 2004, pp. 625–635, 2016.

[18] S. S. Mulani and P. I. Jagad, "Analysis of the Effects of Plaque Deposits on the Blood Flow through Human Artery," *Int. Eng. Res. J.*, vol. 41, no. 2, pp. 2319–3182, 2015.

[19] S. Sriyab, "Mathematical analysis of non-Newtonian blood flow in stenosis narrow arteries," *Comput. Math. Methods Med.*, vol. 2014, no. December 2014, p. 479152, 2014.

[20] M. Dabagh, W. Takabe, P. Jalali, S. White, and H. Jo, "Hemodynamic features in stenosed coronary arteries: CFD analysis based on histological images," *J. Appl. Math.*, vol. 2013, p. 11, 2013.

[21] S. Kamangar *et al.*, "Effect of stenosis on hemodynamics in left coronary artery based on patient-specific CT scan," *Biomed. Mater. Eng.*, vol. 30, no. 4, pp. 463–473, 2019.

[22] R. Tabe, F. Ghalichi, S. Hossainpour, and K. Ghasemzadeh, "Laminar-to-turbulence and relaminarization zones detection by simulation of low Reynolds number turbulent blood flow in large stenosed arteries," *Biomed. Mater. Eng.*, vol. 27, no. 2–3, pp. 119–129, 2016.

[23] S. A. Ahmed and D. P. Giddens, "Pulsatile poststenotic flow studies with laser Doppler anemometry," *J. Biomech.*, vol. 17, no. 9, pp. 695–705, 1984.

[24] F.-F. Zhou, "Coronary Artery Diameter is Inversely Associated with the Severity of Coronary Lesions in Patients Undergoing Coronary Angiography," *Cell. Physiol. Biochem.*, vol. 43, pp. 1247–1257, 2017.

[25] M. G. Rabby, A. Razzak, and M. Molla, "Pulsatile non-Newtonian blood flow through a model of arterial stenosis," *Procedia Eng.*, vol. 56, pp. 225–231, 2013.

[26] A. Buradi and A. Mahalingam, "Effect of stenosis severity on wall shear stress based hemodynamic descriptors using multiphase mixture theory," *J. Appl. Fluid Mech.*, vol. 11, no. 6, pp. 1497–1509, 2018.

[27] E. Doutel, J. Carneiro, J. B. L. M. Campos, and J. M. Miranda, "Experimental and numerical methodology to analyze flows in a coronary bifurcation," *Eur. J. Mech. B/Fluids*, vol. 67, pp. 341–356, 2018.

[28] M. A. Kabir, M. F. Alam, and M. A. Uddin, "A numerical study on the effects of reynolds number on blood flow with spiral velocity through regular arterial stenosis," *Chiang Mai J. Sci.*,

vol. 45, no. 6, pp. 2515–2527, 2018.
[29] I. Ansys, “ANSYS Fluent User ’ s Guide.” 2013.
[30] W. Versteeg, H K; Malalasekera, *An Introduction to Computational Fluid Dynamics, The finite volume method*, Second. Prentice Hall, 2007.